



# Magnetic susceptibility artefact on MRI mimicking lymphadenopathy: description of a nasopharyngeal carcinoma patient

Feng Zhao<sup>1</sup>, Xiaokai Yu<sup>1</sup>, Jiayan Shen<sup>1</sup>, Xinke Li<sup>1</sup>, Guorong Yao<sup>1</sup>, Xiaoli Sun<sup>1</sup>, Fang Wang<sup>1</sup>, Hua Zhou<sup>2</sup>, Zhongjie Lu<sup>1</sup>, Senxiang Yan<sup>1</sup>

<sup>1</sup>Department of Radiation Oncology, <sup>2</sup>Department of Radiology, the First Affiliated Hospital, College of Medicine, Zhejiang University, Hangzhou 310003, China

*Correspondence to:* Zhongjie Lu. Department of Radiation Oncology, the First Affiliated Hospital, College of Medicine, Zhejiang University, Hangzhou, Zhejiang 310003, China. Email: luzhongjie@zju.edu.cn; Senxiang Yan. Department of Radiation Oncology, the First Affiliated Hospital, College of Medicine, Zhejiang University, Hangzhou, Zhejiang 310003, China. Email: yansenxiang@zju.edu.cn.

**Abstract:** This report describes a case involving a 34-year-old male patient with nasopharyngeal carcinoma (NPC) who exhibited the manifestation of lymph node enlargement on magnetic resonance (MR) images due to a magnetic susceptibility artefact (MSA). Initial axial T1-weighted and T2-weighted images acquired before treatment showed a round nodule with hyperintensity in the left retropharyngeal space that mimicked an enlarged cervical lymph node. However, coronal T2-weighted images and subsequent computed tomography (CT) images indicated that this lymph node-like lesion was an MSA caused by the air-bone tissue interface rather than an actual lymph node or another artefact. In addition, for the subsequent MR imaging (MRI), which was performed after chemoradiotherapy (CRT) treatment for NPC, axial MR images also showed an enlarged lymph node-like lesion. This MSA was not observed in a follow-up MRI examination when different MR sequences were used. This finding suggests that when performing lymph node staging for patients with head and neck carcinomas such as NPC, the possibility of an MSA should be considered to avoid misinterpretation and excessive treatment.

**Keywords:** Magnetic resonance imaging (MRI); magnetic susceptibility artefact (MSA); nasopharyngeal carcinoma (NPC); radiotherapy (RT); chemotherapy

Submitted Jun 15, 2017. Accepted for publication Aug 30, 2017.

doi: 10.21037/tcr.2017.09.16

**View this article at:** <http://dx.doi.org/10.21037/tcr.2017.09.16>

## Introduction

Magnetic resonance imaging (MRI) is essential for detecting early nasopharyngeal carcinoma (NPC), staging the primary tumour, and evaluating associated retropharyngeal and cervical lymphadenopathy (1). The assessment of cervical lymph nodes by MRI plays important roles in treatment planning and in monitoring patients after therapy to detect tumour recurrence and radiation-associated changes in soft tissue and bone. Occasionally, artefacts are encountered during MR imaging. Magnetic susceptibility

artefacts (MSAs) are a variety of MRI artefacts that share distortions or local signal change due to local magnetic field inhomogeneities from a variety of compounds (2,3). Generally, metals inside or outside the body can cause local distortions in the static magnetic field that may produce MSAs. Additionally, local magnetic field inhomogeneities may occur at interfaces between tissues with different magnetic susceptibilities, and the resulting local field gradients can produce MSAs. We report a case involving an NPC patient with an unusual MSA that raised suspicions of cervical lymphadenopathy in MR images.

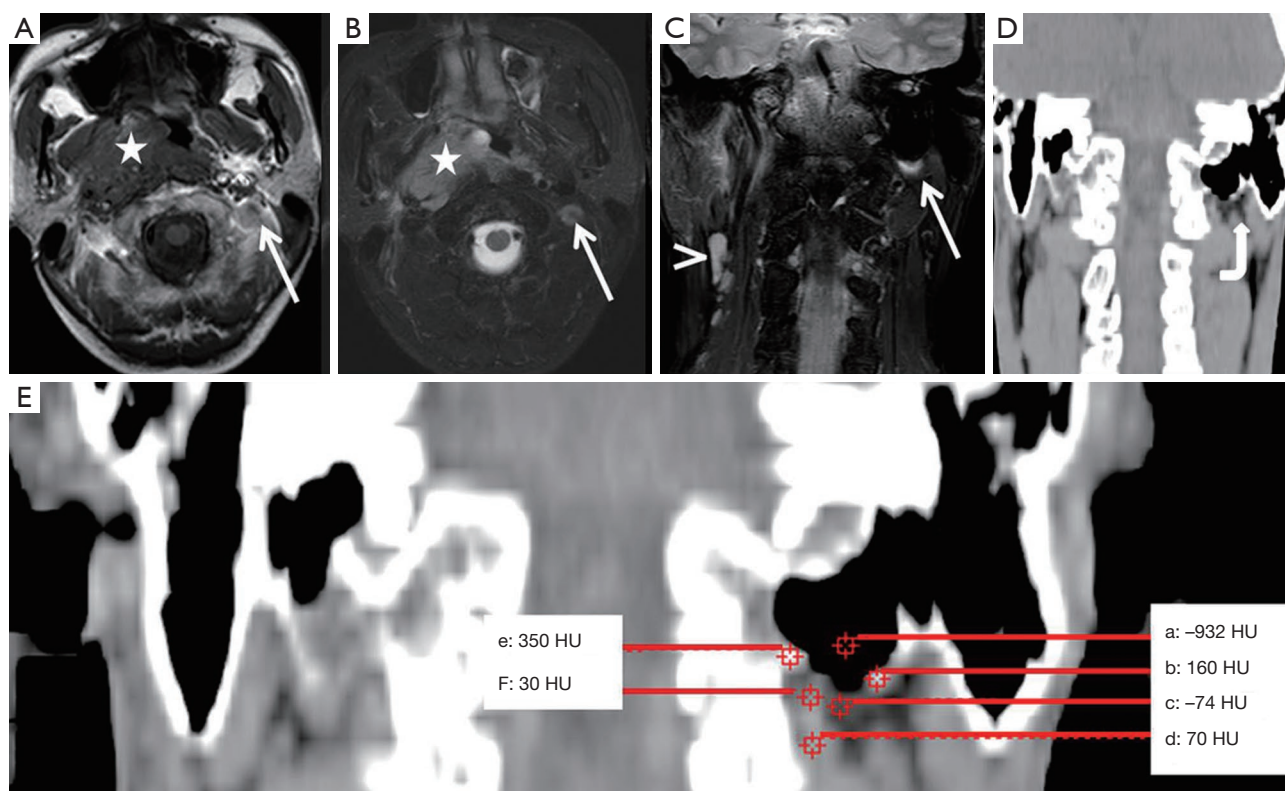


**Figure 1** MR images acquired before treatment for a 34-year-old male patient with nasopharyngeal carcinoma. (A) Axial T1WI-SE MR image (TR =450 ms, TE =10 ms) that reveals a large primary tumour with slight hypointensity in the nasopharynx (star) and appears to show a round nodule with slight hyperintensity in the left retropharyngeal space (arrow); (B) axial T2WI-TSE-SPAIR MR image (TR =3,600 ms, TE =100 ms) reveals a large primary tumour with high intensity in the nasopharynx (star) and appears to show a round nodule with high intensity in the left retropharyngeal space (arrow); (C) coronal T2WI-TSE-SPAIR MR image (TR =1,900 ms, TE =60 ms) reveals an arc-shaped nodule (arrow) with high intensity located under the mastoid air cells and several enlarged cervical lymph nodes (arrowhead) on the right side of the neck; (D) coronal CT image that indicates that the left mastoid cavity had a much larger volume than the right mastoid cavity and that the medial inferior wall extended much further downward for the left mastoid air cells (curved arrow) than for the right mastoid air cells; (E) zoomed-in coronal CT image that indicates that the medial inferior wall of the left mastoid cavity was surrounded by various components with different CT values. TE, echo time; TR, repetition time.

### Case presentation

A 34-year-old man was referred to our institution for the evaluation and management of NPC after undergoing nasopharyngeal biopsy and being pathologically diagnosed with non-keratinising carcinoma. The patient reported a 3-month history of sore throat and nasal discharge stained with blood. Physical examination revealed bilateral cervical lymph node enlargement. The patient underwent MRI (Figure 1) for the evaluation and staging of NPC. This MRI indicated that the primary tumour involved the nasopharynx, parapharyngeal space and hypopharynx, with bilateral metastasis to cervical lymph nodes. In axial T1-

weighted MR images (Figure 1A) and axial T2-weighted MR images (Figure 1B), there was a round nodule with hyperintensity in the left retropharyngeal space; this nodule mimicked an enlarged cervical lymph node. On coronal T2-weighted MR images (Figure 1C), there was a signal void on the left side of the mastoid air cells that was partly surrounded by an arc with high signal intensity. In addition, a coronal computed tomography (CT) image (Figure 1D) showed that the bilateral mastoid regions were cellular in nature with larger portions of air space and that the left mastoid cavity (curved arrow) was much larger than the right mastoid cavity. A zoomed-in coronal CT image showed that the distal portion of the left mastoid cavity

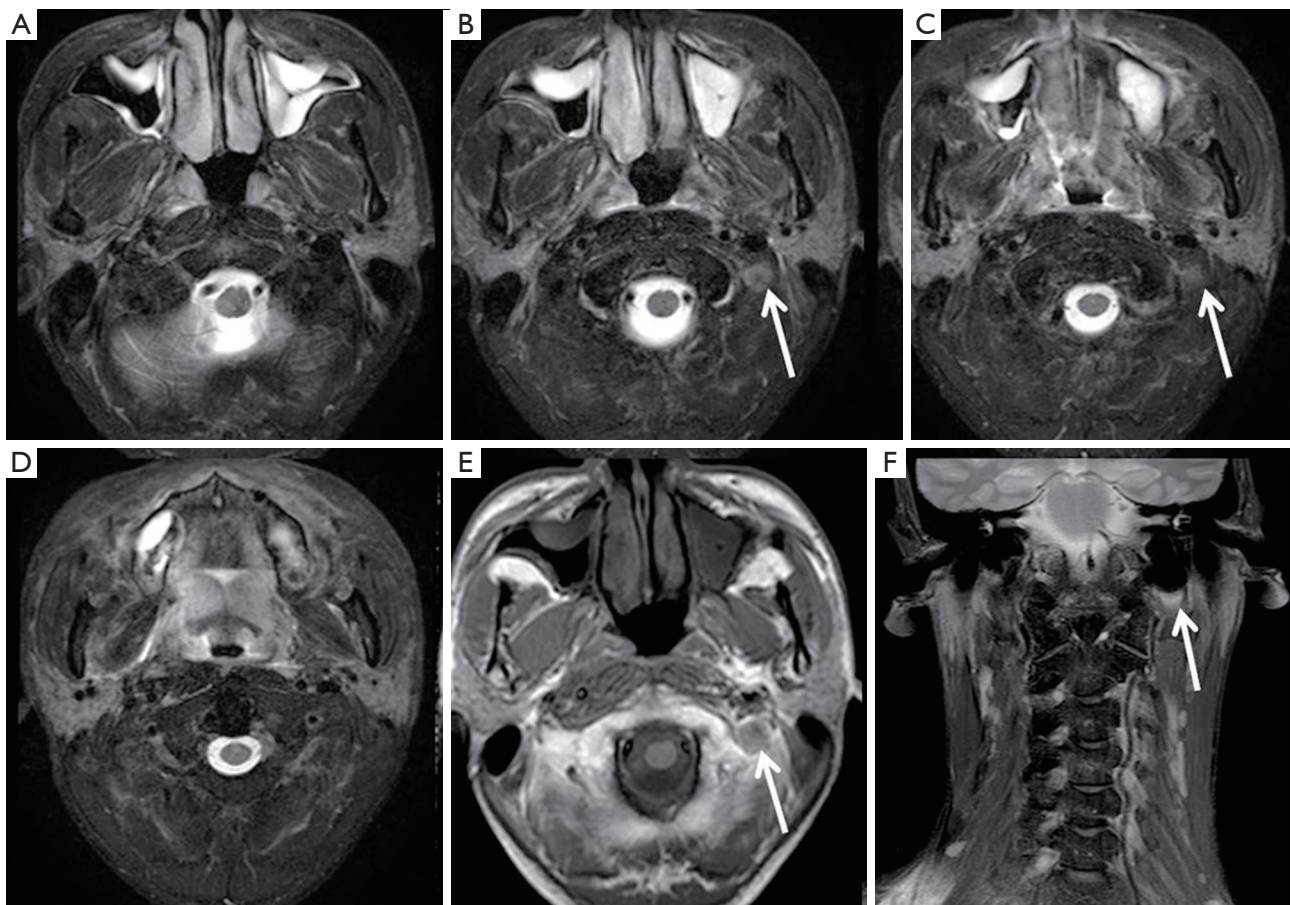


**Figure 2** MR images of the patient acquired after 1 month of CRT. (A-D) Continuous axial T2WI-TSE-SPAIR images (TR =3,600 ms, TE =100 ms) demonstrate that the volume of the primary tumour in the nasopharynx had significantly decreased and appear to show a round nodule with slight hyperintensity in the left retropharyngeal space (B,C) (arrows); (E) axial T1WI-SE MR image (TR =450 ms, TE =10 ms) demonstrates that the volume of the primary tumour in the nasopharynx had significantly decreased and appears to show a round nodule with slight hyperintensity in the left retropharyngeal space (arrow); (F) coronal T2WI-TSE-SPAIR MR image (TR =1,900 ms, TE =60 ms) reveals an arc-shaped nodule (arrow) with high intensity located under the mastoid air cells. No significantly enlarged cervical lymph nodes were observed. CRT, chemoradiotherapy; TE, echo time; TR, repetition time; SPAIR, SPectral Attenuated Inversion Recovery.

was surrounded by various components with different CT signals (*Figure 1E*). All these phenomena indicated that the suspicious lymph node in the axial images was an MSA caused by the air-tissue interface between mastoid air cells and adjacent tissues.

The patient was diagnosed with NPC at stage IVA and treated with concurrent platinum-based chemoradiotherapy (CRT) involving intensity-modulated radiation therapy (IMRT). Radiation therapy was delivered using a simultaneous-integrated IMRT boost technique. A total dose of 6,976 cGy, which was calculated for the planning target volumes of the primary tumour plus any node disease,

was delivered over 32 treatment days. The patient received cisplatin 80 mg/m<sup>2</sup> (i.v.) on days 1, 22, and 43 during IMRT, followed by adjuvant cisplatin (80 mg/m<sup>2</sup>) on day 1 and fluorouracil (1,000 mg/m<sup>2</sup>/d) on days 1 through 4, which was administered every 4 weeks for three cycles.

A follow-up MRI (*Figure 2*) was performed after 1 month of concurrent CRT. The resulting MR images showed that the primary tumour and the metastases in the cervical lymph nodes had resolved but that the MSA located next to the left side of the mastoid remained (*Figure 2B,C,E,F*). Four years after NPC treatment, a follow-up MRI examination (*Figure 3*) was conducted that included a different MR scan

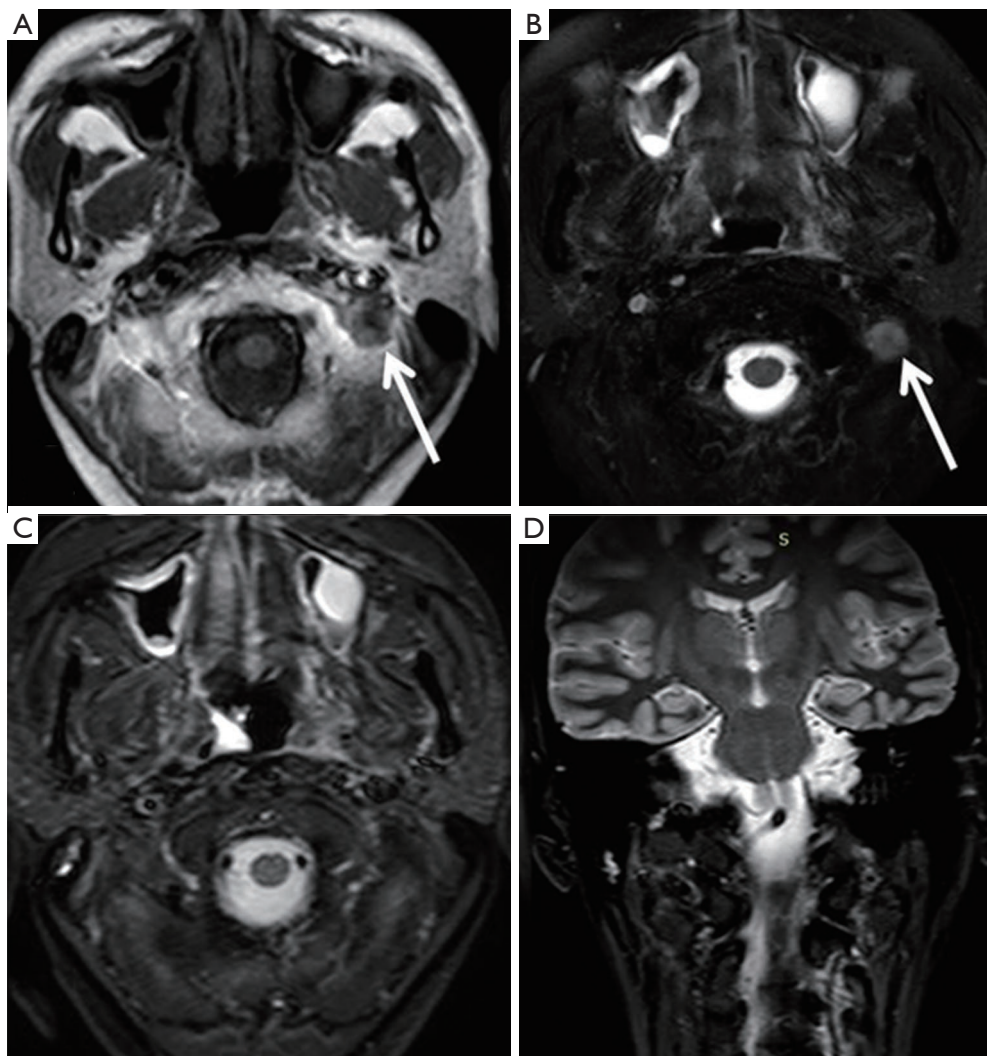


**Figure 3** MR images of the patient acquired approximately 4 years after concurrent chemoradiotherapy and adjuvant chemotherapy. (A) Axial T1WI-SE MR image (TR =450 ms, TE =10 ms) that demonstrates that the volume of the primary tumour in the nasopharynx had significantly decreased and appears to show a round nodule with slight hyperintensity in the left retropharyngeal space (arrow); (B) axial T2WI-TSE-SPAIR MR image (TR =3,600 ms, TE =100 ms) demonstrates that the volume of the primary tumour in the nasopharynx had significantly decreased and appears to show a round nodule with high intensity in the left retropharyngeal space (arrow); (C) axial STIR MR image (TR =2,300 ms, TE =60 ms) in which the round nodule noted in other images was not observed; (D) coronal STIR MR image (TR =2,300 ms, TE =60 ms) in which the round nodule noted in other images was not observed. TE, echo time; TR, repetition time; STIR, Short TI Inversion Recovery; SPAIR, SPectral Attenuated Inversion Recovery.

sequence (Figure 3C,D). On MR images acquired using the parameters that had previously been employed with T2WI-TSE-SPAIR (SPectral Attenuated Inversion Recovery), the MSA that mimicked a lymph node was reproduced (Figure 3A,B); in contrast, on MR images acquired using another fat suppression technique of Short TI Inversion Recovery (STIR), no significant artefacts were detected

(Figure 3C,D).

## Discussion

MRI has been widely used for disease staging. Additionally, MRI has been increasingly used for radiotherapy simulation scans and planning (4,5). However, numerous artefacts and

pseudo-lesions can increase the difficulty of interpreting MRI findings. There are many different types of artefacts, such as MSAs, cerebrospinal fluid (CSF) pulsation artefacts, blood flow artefacts, homogeneity artefacts, motion artefacts, and truncation artefacts (2). MSAs are usually caused by the presence of ferromagnetic materials, such as “metal implants”, given the vast difference in magnetic properties between living human tissue and such implants (6,7). In addition, MSAs are pronounced at interfaces between materials with extremely different susceptibilities that produce large spatial variations in the local magnetic field, such as air-tissue and bone-tissue interfaces (8,9). In our case, the left mastoid cavity had a much larger volume than the right mastoid cavity, and the distal portion of the left mastoid air cells extended downward. Several components surrounded the distal part of the left mastoid cavity, such as bony tissues (b: 160 HU, e: 350 HU), soft tissues (d: 70 HU, f: 30 HU), and fat tissues (c: -74 HU). Therefore, the interface between the mastoid air cells and adjacent soft tissues with various CT values could have disturbed the homogeneity of the local magnetic field and thereby created the MSA seen in MR images. This case illustrated the importance of recognising an MSA when performing MRI and taking the necessary steps to identify the source of this artefact and delimit it. In this case, we relied on coronal MR images and CT images and found that the artefact could be attributed to the air-tissue interface between the left side of mastoid air cells and adjacent tissues. If this MSA had been misdiagnosed as a lymph node, evaluations of response to systemic treatment might have been unreliable, and the patient might have undergone excessive medical treatment, such as surgical lymph node excision or the re-irradiation of local lymph nodes.

As previously reported (2,9-11), approaches to minimising MSAs include adjusting pulse sequence and acquisition parameters to decrease spin dephasing, increasing receiver bandwidth to reduce the relative contribution of signal distortion to the overall image, changing k-space sampling techniques, changing field strength, using smaller voxels, and so on. Specifically, the spin-echo sequence is one of the best ways to reduce susceptibility artefacts. Shortening the echo time (TE) can markedly reduce MSAs by allowing less time for spin dephasing to occur (9). The avoidance of steady-state free precession (SSFP), gradient-echo, and echo-planar sequences in favour of spin-echo and fast spin-echo sequences may also reduce MSAs (2,10,11). The STIR sequence is relatively insensitive to magnetic field

inhomogeneity (9,12). Thus, in our case, we changed the MR scan parameters in a follow-up MRI (changed T2WI-TSE-SPAIR sequence to STIR sequence) and successfully eliminated the MSA.

In conclusion, radiologists and physicians should be aware of the possible appearance of lymph node-like MSAs on MR images to avoid misinterpretation and excessive treatment.

### Acknowledgments

*Funding:* This study was funded by grants from the Zhejiang Provincial Natural Science Foundation of China (LQ15H180001, LY16H160013, and LY17H180001) and Zhejiang Province Science and Technology Department Non-profit Program (2014C33199).

### Footnote

*Provenance and Peer Review:* This article was commissioned by the Guest Editors (Yi-Xiang J. Wang, Yong Wang) for the series “Translational Imaging in Cancer Patient Care” published in *Translational Cancer Research*. The article has undergone external peer review.

*Conflicts of Interest:* All authors have completed the ICMJE uniform disclosure form (available at <http://dx.doi.org/10.21037/tcr.2017.09.16>). The series “Translational Imaging in Cancer Patient Care” was commissioned by the editorial office without any funding or sponsorship. The authors have no other conflicts of interest to declare.

*Ethical statement:* The authors are accountable for all aspects of the work in ensuring that questions related to the accuracy or integrity of any part of the work are appropriately investigated and resolved. All procedures performed in study involving human participants were in accordance with the ethical standards of the institutional and/or national research committee(s) and with the Declaration of Helsinki (as revised in 2013). Written informed consent was obtained from the patient for publication of this manuscript and any accompanying images.

*Open Access Statement:* This is an Open Access article distributed in accordance with the Creative Commons Attribution-NonCommercial-NoDerivs 4.0 International License (CC BY-NC-ND 4.0), which permits the non-

commercial replication and distribution of the article with the strict proviso that no changes or edits are made and the original work is properly cited (including links to both the formal publication through the relevant DOI and the license). See: <https://creativecommons.org/licenses/by-nc-nd/4.0/>.

## References

1. Abdel Khalek Abdel Razek A, King A. MRI and CT of nasopharyngeal carcinoma. *AJR Am J Roentgenol* 2012;198:11-8.
2. Vargas MI, Delavelle J, Kohler R, et al. Brain and spine MRI artifacts at 3Tesla. *J Neuroradiol* 2009;36:74-81.
3. Savranlar A, Vurdem ÜE, İnci ME, et al. MR susceptibility artifact due to occupational cause: an unusual case. *Magn Reson Imaging* 2012;30:148-50.
4. Wong OL, Yuan J, Yu SK, et al. Image quality assessment of a 1.5T dedicated magnetic resonance-simulator for radiotherapy with a flexible radio frequency coil setting using the standard American College of Radiology magnetic resonance imaging phantom test. *Quant Imaging Med Surg* 2017;7:205-14.
5. Yuan J, Lo G, King AD. Functional magnetic resonance imaging techniques and their development for radiation therapy planning and monitoring in the head and neck cancers. *Quant Imaging Med Surg* 2016;6:430-48.
6. Choudhri AF, Patel BJ, Phillips ME, et al. Diamagnetic susceptibility artifact associated with graphite foreign body of the orbit. *Ophthal Plast Reconstr Surg* 2013;29:e105-7.
7. Senol S, Gumus K. A rare incidence of metal artifact on MRI. *Quant Imaging Med Surg* 2017;7:142-3.
8. Jordanov MI, Block JJ. Minute amounts of intraarticular gas mimicking torn discoid lateral menisci. *J Magn Reson Imaging* 2010;31:698-702.
9. Huang SY, Seethamraju RT, Patel P, et al. Body MR Imaging: Artifacts, k-Space, and Solutions. *Radiographics* 2015;35:1439-60.
10. Cook SC, Shull J, Pickworth-Pierce K, et al. An unusual cause of susceptibility artifact in magnetic resonance imaging. *J Magn Reson Imaging* 2006;24:1148-50.
11. Shmueli K, Thomas DL, Ordidge RJ. Design, construction and evaluation of an anthropomorphic head phantom with realistic susceptibility artifacts. *J Magn Reson Imaging* 2007;26:202-7.
12. Del Grande F, Santini F, Herzka DA, et al. Fat-suppression techniques for 3-T MR imaging of the musculoskeletal system. *Radiographics* 2014;34:217-33.

**Cite this article as:** Zhao F, Yu X, Shen J, Li X, Yao G, Sun X, Wang F, Zhou H, Lu Z, Yan S. Magnetic susceptibility artefact on MRI mimicking lymphadenopathy: description of a nasopharyngeal carcinoma patient. *Transl Cancer Res* 2017;6(6):1156-1161. doi: 10.21037/tcr.2017.09.16